

# Reduction AWGN from Digital Images Using A New Local Optimal Low Rank Approximation Method

Sadegh Kalantari<sup>1\*</sup>, Mehdi Ramezani<sup>2</sup>, Ali Madadi<sup>3</sup>, Vania V. Estrela<sup>4</sup>, G. G. Oliveira, A.C. B. Monteiro, R. P. Franca, Y. Iano,

<sup>1</sup>Ph.D Student, Faculty of Electrical Engineering, Control Group, University of Tafresh, Tafresh, Iran,  
Email: sadeghkalantari@tafreshu.ac.ir

<sup>2</sup>Assistant Professor, Faculty of Electrical Engineering, Control Group, University of Tafresh, Tafresh, Iran,  
Email: ramezani@tafreshu.ac.ir

<sup>3</sup>Associate Professor, Faculty of Electrical Engineering, Control Group, University of Tafresh, Tafresh, Iran,  
Email: madadi@tafreshu.ac.ir

<sup>3</sup>Dep. of Telecommunications, Fluminense Federal University (UFF),  
Niteroi, RJ, Brazil vania.estrela.phd@ieee.org

<sup>3</sup>School of Electrical and Computer Engineering (FEEC),  
University of Campinas  
Campinas - SP, Brazil,

Email: oliveiragomesgabriel@live.com

Email: carol94monteiro@gmail.com

Email: reinaldopadilha@live.com

Email: yuzo@decom.fee.unicamp.br

## Abstract:

In this paper, image noise reduction is formulated as an optimization problem. The target image is denoised using low rank approximation of a matrix. Considering the fact that the smaller pieces of the picture in natural images are more similar to each other (more dependent); therefore, the use of low rank approximation on smaller pieces of the image is more justifiable. In the proposed method, the image corrupted with AWGN (Additive White Gaussian Noise) is locally denoised, and the optimization problem of low rank approximation is solved on all the patches with fixed sizes. Therefore, for practical purposes, the proposed method can be implemented parallelly. This is one of the advantages of such methods. In all noise reduction methods, the two factors including the amount of the noise removed from the image and the preservation of the edges (vital details) are very important. In the proposed method, the use of TI image (Training Image) obtained from noisy image, the use of SVD adaptive basis, ability to iterate the algorithm and ideas like patch labeling have all lead to sharper results, good edge preservation and acceptable speed compared to the other tested methods.

**Keywords:** Optimal Low Rank Approximation , SVD, Signal Denoising, Image Denoising, Signal Processing.

## 1. Introduction:

Signal denoising is one of the most important issues in the field of digital image processing. Noise destroys or damages vital information and details of a signal. Therefore, noise cancellation is one of the early stages of the process of features extraction, object recognition, image matching, and so on. So far, several methods have been proposed for removing noise from digital images[1-12]. AWGN is one of the most significant noises studied by researchers. In each pixel of noisy image built by AWGN, a value is added to the gray level of the pixel. This value is

sampled independently from Gaussian distribution. AWGN denoising methods can be divided into three categories including correlation-based (or spatial filter), transform-based and hybrid methods. Correlation-based methods work directly with spatial values of the image in the spatial domain. The advantages of correlation-based methods include simplicity of its algorithms and their acceptable speed. Transform-based methods first transfer the image to the desired transform domain and then denoise the image. It can be deduced that applying transformation on a signal means changing the axes of the coordinates to represent the signal. Changing the coordinates of the signal representation, makes it possible to effectively separate the noisy and non-noisy part of the signal that it is the advantages of these methods. The hybrid methods use both of these methods simultaneously and benefit from each one.

When denoising the image, amount of noise eliminated, edge and textures preservation of the image are the most important issues. Two methods of moving average and Gaussian filter are one of the easiest correlation-based methods, which like a low pass filter, soften the high-frequency parts of the image (including noise and edges) and, in addition to noise cancellation, eliminate some of the tiny and vital information of the image [2]. BF(Bilateral Filter) is introduced to better edge preservation [3]. In this filter the value of each pixel is estimated by the average weights of the neighbors that the weights are determined by similarity of intensity and spatial similarity. The NLM method is non-local version of BF which estimates the value of each pixel with the weighted average of the similar pixels of the image that the weights being determined by the similarity between them. The advantages of such methods are the simplicity of the algorithm and the relatively convenient speed of the method.

Transform-based methods are based on the principle that images can be represented by some of the sparse basis like Wavelet, Curvelet and Contourlet [13]. Some of these basis are fixed, but some are adapted to the signal information that selected adaptively. Because of complex singularities in many images, using fixed basis such as wavelet will not always yield acceptable results. Two methods [14] and [15] have proposed an adaptive representation method called K-SVD. In these methods, an optimization problem is solved with greedy algorithms and then a dictionary for noise cancellation can be trained that the columns (atoms) of this dictionary can be used as adaptive basis for sparse representation. Today, the use of methods based on sparse representation in many applications such as noise cancellation, super-resolution, image reconstruction, inpainting, and so on, has provided acceptable results [16-18]. Noise spreads over all transform coefficients. However, most of the basic image information is focused only on a few of the largest coefficients. Hence, in such methods image denoising can be done with many shrinkage methods such as [19]. In general, methods such as K-SVD, [20] and [21] that solve an optimization problem to denoise an image are called optimization-based methods. These methods are commonly found in the family of transform-based methods. Because of solving optimization problems, these methods usually have a lot of computational complexity and are slow.

The BM3D method is one of the hybrid methods that use spatial filtering and transform-based methods [22]. This method denoises the image by grouping similar patches in 3d arrays and sparse filtering. So far, more complete versions of BM3D method have been presented that with

shape-adaptive principal component analysis has improved its results [23]. Some of the hybrid methods like ASVD and SAIST have used useful properties of SVD basis. ASVD method uses SVD for training basis for representing image patches and SAIST method denoises image by using SVD and sparse representing of image patches [24, 25]. The important features of these methods are that they combine the useful properties of correlation-based and transform based methods and output images provide better results in terms of speed and quality.

In this paper, we intend to provide a adaptive local denoising method using adaptive SVD basis. In this method, a TI(Training Image) is created using noisy image and Gaussian filter that its information is used in denoising [26, 27]. According to locality of the algorithm, SVD is computed for all image patches(overlapping) and using TI information each patch is denoised individually and adaptively. In order to prevent artifacts, after computing estimated patches, aggregation phase is done and average obtained values replaced in overlapping areas. One of the advantages of these methods is to deal with each patch individually and can be implemented in parallel in practical purposes. Given the ideas in the proposed method, this method belongs to the family of hybrid methods.

The various sections of the article are as follows. In section 2, we will examine the linear representation of the image using SVD and how to formulate the low rank approximation problem. In section 3, the proposed method will be presented and we will explain the applied ideas. In section 4, the results of the proposed method are presented and conclusions are made in section 5.

## 2. An Overview of SVD Concepts and Low Rank Approximation

### 2.1 An Overview of SVD

Suppose A represents an gray level image. The basic principle of the linear representation of the image is that the matrix A can be represented as the sum of the weighted basis given as equation (1). In this equation,  $a_i$  are the coefficients and  $f_i$  are corresponding basis. These basis can be chosen from well-known basis such as wavelet, curvelet, bandlet, contourlet and so on[28-31].

$$A = \sum_{i=1}^N a_i f_i \quad (1)$$

It is similar to the Fourier series. Each periodic 2d function can be represented in terms of exponential basis and  $C_{mn}$  coefficients are according equation (2).

$$f(x,y) = \sum_{n=-\infty}^{+\infty} \sum_{m=-\infty}^{+\infty} C_{mn} e^{\frac{inpx}{a}} e^{\frac{impy}{b}} \quad , \quad -a < x < a, -b < y < b \quad (2)$$

$$C_{mn} = \frac{1}{ab} \int_{-a}^a \int_{-b}^b f(x,y) e^{-\frac{inpx}{a}} e^{-\frac{impy}{b}} dx dy$$

According to the expansion of the Riemann–Lebesgue lemma,  $C_{mn}$  coefficients are descending and equation (3) results [32].

$$\lim_{m \rightarrow \infty} \lim_{n \rightarrow \infty} C_{mn} = 0 \quad (3)$$

This lemma states that the high harmonic coefficients are very small and they have very little effect on reconstructing the signal. So, if we truncate coefficients from a frequency to the next, the original signal can be reconstructed with a fairly good approximation. In the next section, we will use the idea of truncating some of the coefficients for signal denoising using SVD.

In SVD theory, each matrix can be decomposed as equation (4):

$$A = USV^t \quad (4)$$

That  $U_{m \times m} = [u_1 \dots u_m]$  (left singular vector) and  $V_{n \times n} = [v_1 \dots v_n]$  (right singular vector) are orthogonal matrix. So according to equation (5):

$$VV^t = V^tV = I_n, \quad UU^t = U^tU = I_m. \quad (5)$$

It should be noted that the columns of  $U_{m \times m}$  and  $V_{n \times n}$  matrices are composed of  $AA^t$  and  $A^tA$  orthonormal eigenvectors matrices respectively.  $S_{m \times n}$  is a semi-diagonal matrix that the values on its diagonal are the singular values of the  $A^tA$  or  $AA^t$  matrices. So we will have:

$$S_{m \times n} = \text{diag}(s_1, \dots, s_p), \quad p = \min\{m, n\} \\ s_1 \geq s_2 \geq \dots \geq s_k > 0, s_{k+1} = \dots = s_p = 0 \quad (6)$$

That  $s_1$  is the largest and  $s_k$  is the smallest non-zero singular value of the matrix A.

## 2.2 The Formulation of Low Rank Approximation Problem

Approximation of a matrix with a lower rank matrix can be done using SVD. The main issue in this section is to estimate the low rank matrix B from the matrix A. According to equation (7), in singular value decomposition of matrix A with rank r we will have:

$$A = [U_1 | U_2] \begin{bmatrix} s_1 & 0 & 0 & \dots \\ 0 & 0 & 0 & \dots \\ \vdots & \vdots & \vdots & \vdots \\ 0 & 0 & s_r & \dots \\ \vdots & \vdots & 0 & \dots \\ 0 & 0 & 0 & \dots \end{bmatrix} \begin{bmatrix} v_1^t \\ v_2^t \\ \vdots \\ v_r^t \\ \vdots \\ \vdots \end{bmatrix}, \quad \text{rank}(A) = r \quad (7)$$

Due to definition of the two matrices  $U$  and  $V$  in section 2.1, the singular value decomposition of the matrix A can be represent as equation (8):

$$A = u_1 s_1 v_1^t + u_2 s_2 v_2^t + \dots + u_r s_r v_r^t, \quad s_1 > s_2 > \dots > s_r. \quad (8)$$





are shown in Figure 1. It should be noted that in these tests, the number of samples is 100 that arranged in a  $10 \times 10$  matrix. In the following tests,  $k$  is sparsity of the semidiagonal matrix  $S$  that it is determined using Eckart-Young-Mirsky criterion. For example,  $k=3$  means that the signal is reconstructed by 3 of the largest singular values(is denoised). The following results show that, truncating smaller singular values has improved the noisy signals.

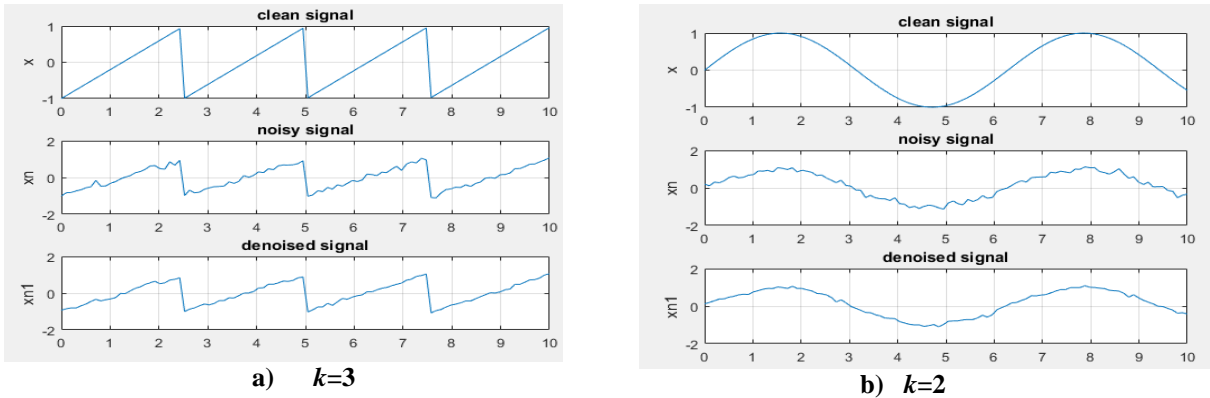


**Figure 1.** The results of applying noise reduction method using SVD and Eckart-Young-Mirsky criterion on two noisy signals.

### 3. The Proposed Method

Before explaining the proposed method, in order to better understanding the cause of the used ideas and more detailed description of the proposed method, we need to review some of the basics used in the proposed method.

#### 3.1 A review of the Gaussian Filter, High and Low Frequency Component and Canny Edge Detection Method

##### 3.1.1 2d Gaussian Filter

2d Gaussian filter is a low pass filter based on probability distribution function of (17).

$$f(x,y) = \frac{e^{-\frac{x^2+y^2}{2s_g^2}}}{2ps_g^2} \quad (17)$$

In Figure 2, a view of 2d Gaussian filter is depicted. In the above equation,  $s_g$  is the Gaussian filter standard deviation and  $x$  and  $y$  representing the filter locations. Gaussian filter is a low pass filter. Due to the fact that noise appears at high frequencies in the image, image denoising using Gaussian filter is one of the easiest ways. After applying it to the image, the high-frequency parts of the image (edges + details) and noise somewhat destroyed and the remaining parts are general and smooth parts of the image. In fact, the resulted image is smoothed(blured).

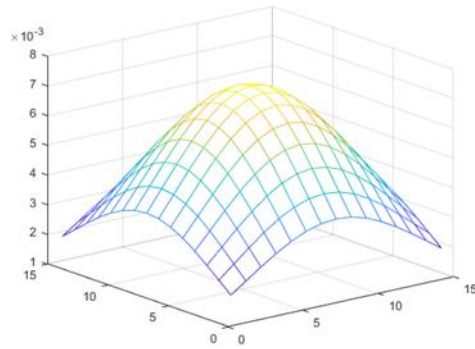


**Figure 2. 2d Gaussian filter with window size=15 and the standard deviation=6.**

For example, when the CAMERAMAN image passes through a Gaussian filter with a standard deviation of 2, the resulting image will be in accordance with Figures 3 and 4. As can be seen from Figures 3 and 4, the blur effect of the Gaussian filter to eliminate noise is an unpleasant factor that results in the loss of many details of the image. Using this filter, we can decompose the high frequency and the low frequency component of the image, which we will examine in the next section.



**Input Image**



**Gaussian filter output image with standard deviation 2**

**Figure 3. Effect of Gaussian filter on CAMERAMAN image**



**Input Noisy Image**



**Gaussian filter output denoised image with standard deviation 2**

**Figure 4. Effect of Gaussian filter on CAMERAMAN image**

### 3.1.2 Decomposition of High Frequency and Low Frequency Component of Image Using Gaussian Filter

In general, each image can be decomposed into sum of a low-frequency image (general details) and a high-frequency image (including edges and fine details). For example, Figures 5 and 6 illustrate the decomposition of an noisy image and non-noisy image into two high frequency and low frequency images, respectively.

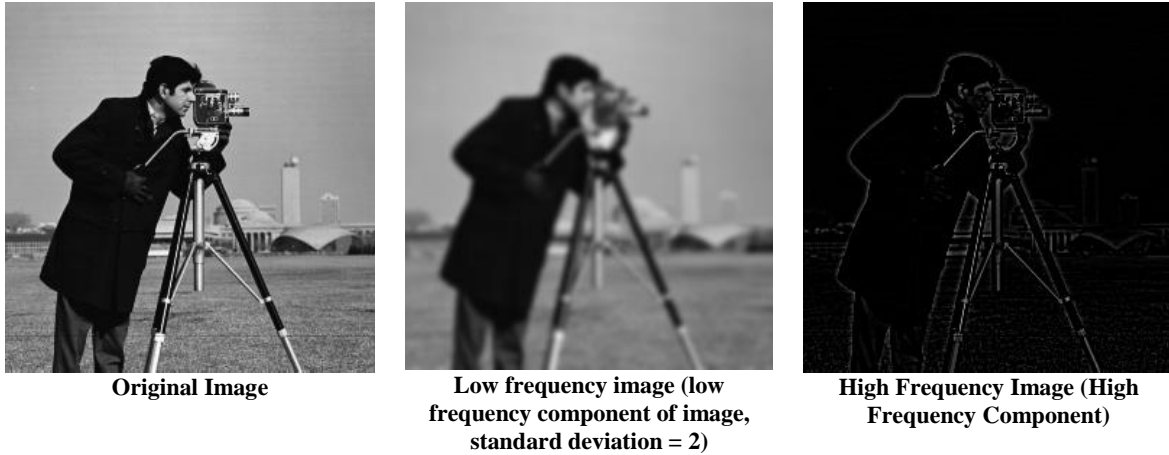


**Figure 5. Decomposing the low frequency and high frequency component of the image using the Gaussian filter**

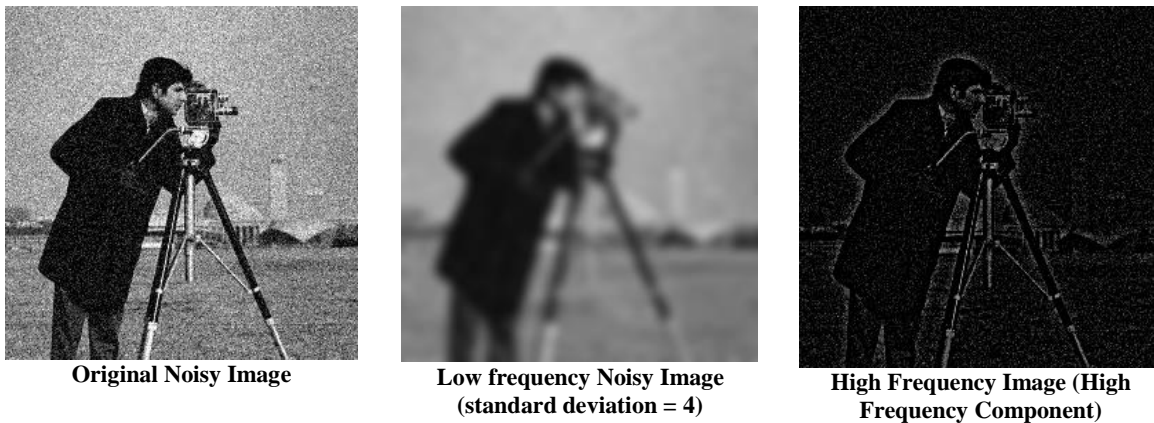


**Figure 6. Decomposing of low frequency and high frequency component of Noisy image using Gaussian filter**

By separating the high frequency and the low frequency component of the image using the Gaussian filter, we will be able to separate the noise+edge image (the high frequency component of the image) in the noisy images. Then by using the information of low frequency component that contains general information of the image, the noise+edge image is denoised, and ultimately, by integrating the denoised high frequency component, and the low frequency component, we obtain an image without noise. Using this idea, we use the information we get from the image itself, and we can obtain a higher accuracy in the process of truncating the SVD coefficients.

Because according to the analysis, the larger coefficients of (low frequencies) SVD, contain image generalizations, and smaller coefficients (high frequencies) include image and noise details. Now, if we can truncate the coefficients adaptively using low frequency component information, the output image will have an acceptable sharpness in addition to noise removal.

### 3.1.3 Canny Edge Detection Method

Canny Edge Detection is one of the most common methods for extracting the Image edges. In this method, first the magnitude and direction of the gradient of the image are calculated at each point. Then using the information of the gradient, two thresholds (low and high) are considered. The points of the image whose gradients are higher than the upper threshold are definitely among the strong edges, but the points whose gradients are lower than the lower threshold are not considered to be edges of the image. The points that their gradients are between the two thresholds are considered to be one of the edges where their neighbors are the edges of the image. This method has acceptable accuracy compared to other methods and at the same time, using two thresholds for the image gradient, extracts the strong and weak edges of the image. In Figures 7 and 8, we can see an example of the edge detection with canny method for noisy and non-noisy images.



Original Image



Edge detection using Canny method

Figure 7. Edge detection for CAMERAMAN image using Canny method



Original Noisy Image



Edge detection using Canny method

Figure 7. Edge detection for CAMERAMAN image using Canny method

As deduced from Figure 8, the derivation(edge detection) of a noisy image results in the creation of another noisy image. For better understanding of this issue, consider Figure 9.

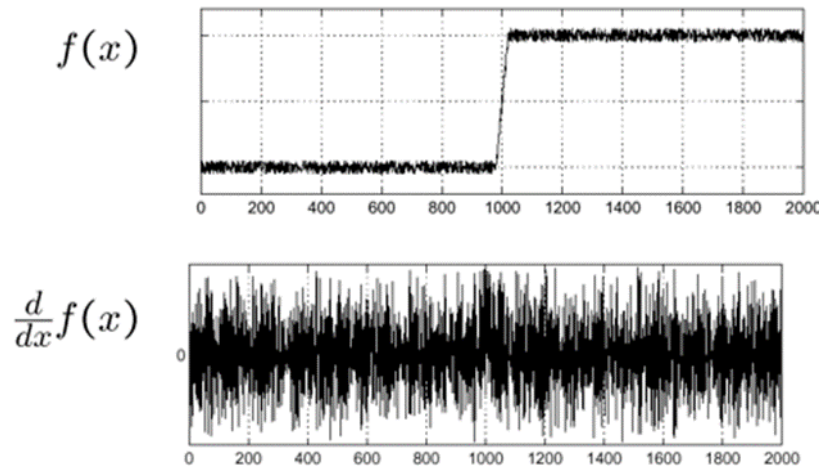


Figure 9. derivation of a noisy signal

The above result is obtained if a noisy signal is derived for the edge detection(structures and textures areas that have sudden changes). So, the derivation of the resulting signal will be noisy and can not be used to identify the edges. In order to prevent this problem, the signal must be smoothed. That is, it is passed through a low pass filter (Gaussian filter) so that the high-frequency components that cause the problem become less effective and then derivate it to reveal the edges. In Figure 10, this process is depicted for a noisy signal. In Figure 10,  $f$  is the noisy signal and  $h$  refers to a Gaussian filter. Given the AWGN noise and the definition of the standard deviation calculation, in this paper, the standard deviation of the Gaussian filter for each image is estimated using Equation (18).

$$s = \frac{\sum_{i=1}^m \sum_{j=1}^n (a_{ij} - m_A)^2}{m \cdot n}, \quad m_A = 0. \quad (18)$$

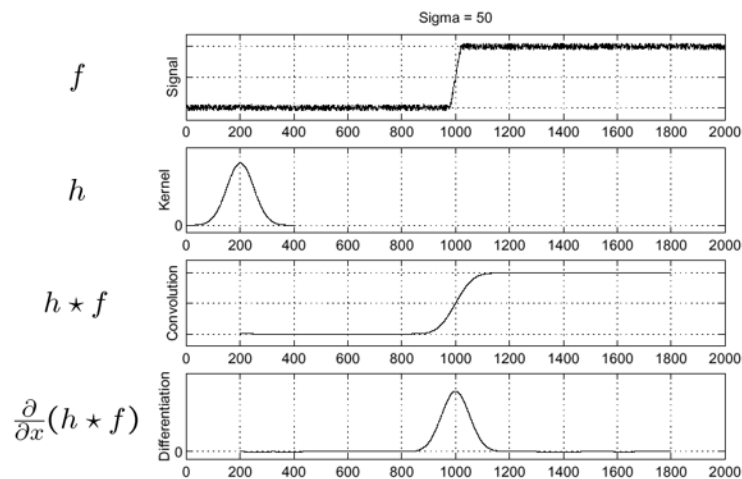


Figure 10. How to use a derivative of a noisy signal to identify the edge

For the reasons given, to identify the edges and structured areas in the image, first we pass the image from a low pass filter to minimize the effects of noise, then it is derived (canny algorithm) and we find the edges of the image. In Figure 11, these steps are shown.



Noisy Image



Low frequency component of noisy image with  $w=15$  and standard deviation=6.



Extracted edges using canny method



Noise + Image edges

Figure 11. Production of TI and Noise+Edges image from a noisy image

As we can see from the above, using the idea of filtering the image with Gaussian filters and then extracting the edge using the low-frequency component of the image, we were able to detect the critical edges of the image (Training Image) with acceptable accuracy. We will use the information in the training image to remove noise from the noise + edge image. After denoising of noise+edge image, it will be combined with the low-frequency component of the image and create a denoised image.

### 3.2 Using Training Image and Algorithm of the proposed method

In the previous section we were able to determine the edge image(important parts of the image structures) using a Gaussian filter from the noisy image. The resulting image can be used as an training image, or as a model for detection of texured areas of the image. The resulting TI makes

it possible to use the information in the noisy image to eliminate noise adaptively. In this section, based on the reviewed basics and ideas, a new algorithm is proposed that, in addition to eliminating noise in smooth areas, improves the output image sharpness. According to the previous descriptions, the proposed method is shown in table 1. As can be deduced from Figure 12, some noise reduction methods eliminate many of the critical details of the image and blur the output image.

As described in previous sections, we would like to apply low rank approximation to smaller pieces of the image. The reason is that the smaller parts in a natural image are more similar to each other, and low rank approximation of smaller pieces of the image is more justifiable. For this purpose, for each piece extracted from the image (the high frequency component of the noisy image), the singular value decomposition of that slice is calculated. In order to better preserve the edges and important details of the image, using the corresponding patches in the TI image, We make pieces of noisy image that have low edges (that is, the part of the image is almost smooth) to be reconstructed with smaller singular values and we will compel the parts that are more detailed to be made with a greater number of singular values. For this purpose, in the proposed algorithm, for each patch of the noisy image, the corresponding patch in the TI image is also extracted. If the average gradient in each patch exceeds the mean gradient of the total TI image, it indicates that the patch belongs to the textured parts of the image, and so we use the ECKERT method to truncate and determine k. If the average gradient of the patch was less than the mean gradient of the total TI image, it indicates that the patch belongs to the smooth areas of the image and in order to reduce the computational complexity, the k value is considered to be 1. This idea, in addition to reducing the computational complexity, preserves important and vital information in structured areas and prevents the image from blurring. This operation is performed on all the extracted patches of the noisy image (with overlapping) and eventually the denoised image is created. It should be noted that with respect to the overlapping of patches with each other, there are several values for parts of the image. In those parts, the mean of those values is used and that's called Aggregation process. Since the optimization problem is solved in the noise reduction process of the proposed method, the proposed method is one of the optimization-based combination methods. In order to reduce the computational complexity and increase the speed of the proposed algorithm, the patches of the image are labeled in terms of their similarity (patch labeling process). Therefore, before entering the low rank approximation process, in the preprocessing stage, the similarity of different patches of the TI image is examined using Euclidean distance, and the patches that are similar to each other have the same label. Using Equation 19, we can examine the similarity of each patch with other patches:

$$s(p_i, p_c) = \|p_i - p_c\|_2^2 \quad (19)$$

In the above equation,  $\| \cdot \|_2$  refers to Euclidean distance,  $p_i$  refers to vectorized reference patch, and  $p_c$  refers to vectorized candidate patch. The smaller the value of  $s(p_i, p_c)$  means that the two patches are more similar to each other. The reference patch with n numbers of the same patches together make up a group that they all have the same label. By labeling different TI patches and using the above idea, the computational complexity of the proposed method is reduced and for

the patches of each group, the k value is considered to be the same. In fact, the k value is calculated for the agent of each group and for other patches of the group, the same k is considered.

Another idea that can be improve the image quality is that the proposed method can be iterative. By performing the above steps on the noisy image(in the first iteration) and denoised image(in the next iteration), the output image is refined and the noise effects will be minimized. Of course, this idea will increase the quality of the output image for a limited number of iterations and will not have any effect on the output image from a iteration number to the next.



**Figure 12. the result of method [20]**

<p>Input: Noisy Image A  Output: Denoised Image H  Parameters: ws:Patch Size, n:The Number of Groups in Patchlabeling, iternum:The number of Iteration.</p> <p><b>Algorithm:</b>  Set ws and n.  For iter=1 to iternum do  1-Decompose <math>A</math> for first iteration and H for other iteration to <math>A_L</math> (Low Frequency Component) and <math>A_H</math> (High Frequency Component) Using Part 3.  2- Get the TI Image Using CANNY Edge detection and <math>A_L</math> .  3- Do Patch Labeling on the TI with n Group Using Part 3.2.  4-For all of the Patches with ws size in <math>A_H</math> , Extract the Corresponding Patch in the TI Image. For Patches with the same label, set the value of k equal to specified value fo their agent and go to step 6 .  5-If the Mean Gradient of the Patch is greater than the average gradient of the image, set k with ECKERT Method, Otherwise set k equal to 1.  6-Reconstruct the Patch with specified k and Place it in the Corresponding Location in Denoised Image <math>H_H</math> .  7-Do Aggregation phase.  8-Compute Denoised Image with following equation : <math>H = H_H + A_L</math></p>
<b>Table 1. The proposed method</b>

#### 4. The Results of The Proposed Method

Given that the proposed method which is one of the optimization-based combination methods, In this section, the results of the proposed method are compared with the methods [18], [19],[6],[11] and [21]. The above methods are implemented on the standard test images of CAMERAMAN, LENA, PEPPERS, Mandrill, Boats and the performance of each one will be investigated. The reason for using these standard images is their variability in texture and detail, and most articles in this field evaluate the effectiveness of the proposed method on these images. Implementation of all algorithms are done using a computer with an Intel Corei7.1.8GH

processor, 6GB of RAM and with the MATLAB software running under the Windows 8.1 operating system. In this section, in all experiments, the size of the CAMERAMAN image is  $256 \times 256$ , the size of the rest of Images is  $512 \times 512$ , and the noisy image is obtained by adding the AWGN with various  $\sigma_n$  to test images. To test the performance of the proposed method, as well as articles in Image Processing, the PSNR (Peak Signal-to-Noise Ratio) and FSIM (Feature Similarity Index) criteria have been used. These two criteria are fully stated in the reference method [11] and they have not been repeated in this article. Although the PSNR criterion is calculated in all noise-canceling methods, in some cases the quantity obtained does not correspond to human visual perception. For this purpose, in addition to the PSNR, another measure called FSIM is used. This criterion is obtained by measuring the similarity between the two images and by combining the phase correlation property and the gradient magnitude. The results of one method for each of the above criteria are superior to the other methods if they have a higher numerical value.

For proper selection of algorithm parameters such as  $n$ , number of Iterations, and patch size, the proposed method has been tested on the CAMERAMAN image and its results are reported in Table 2. According to the results of Table 2 and Figure 13, for the proposed method,  $ws = 25$ ,  $n = 1000$  and  $iternum = 3$  are considered, and Its results, along with other methods, are presented in Table 3 and Figure 14. In order to investigate the performance of ideas such as being local and choosing an adaptive optimal  $k$  in the proposed method, It's results are presented globally and with various sparsity in Figure 15. As it is deduced, the above ideas in terms of visual and PSNR criterion have improved the algorithm. Because the results obtained using the above ideas are significantly superior to other comparisons in terms of visual quality (sharpness of image and removing noise) and PSNR criterion.

To test the speed, the proposed algorithm and the compared algorithms are compared in terms of runtime in the same conditions and the results are presented in Table 4. As expected, the reference methods [6], [18] and [19] are slower than the proposed method because they are among the optimization-based methods. The method [11] has a close runtime because of its similarity of with the proposed method. The method [21] is also slower than the proposed method due to the technique used to group similar patches into three-dimensional arrays.

Also, according to the results obtained in this section, the proposed method provides better results in terms of PSNR, FSIM and edge preservation compared to the other methods. The reason is the use of TI obtained from the noisy image in order to determine optimal  $k$ , which helps to maintain useful details in the textured parts of the image. Since the proposed method is one of the optimization-based hybrid methods, it is expected that the execution time of the algorithm will be longer than other methods. But, due to the use of the of patch labeling idea, and by using the same sparsity for similar patches, the computational complexity of the proposed method has been greatly reduced, and the speed of the proposed algorithm is acceptable comared to other methods. Therefore, based on the ideas of local adaptive Svd basis, the training image, patch labeling and the repeatability of the proposed method, the proposed method was able to provide an acceptable performance in terms of quantitative and visual evaluation and speed of algorithm compared to the comparison methods.

n	Patch Size (ws)	PSNR(dB)
500	9	34.17
500	17	34.32
500	25	34.22
500	35	34.07
1000	9	<b>34.37</b>
1000	17	<b>34.44</b>
1000	25	<b>34.54</b>
1000	35	<b>34.28</b>
2000	9	34.2
2000	17	34.31
2000	25	34.15
2000	35	34.11
3000	9	34.11
3000	17	34.12
3000	25	34.04
3000	35	34.01

**Table 2. Analyze the sensitivity of the proposed method parameters on the CAMERAMAN image with  $\sigma_n = 10$**

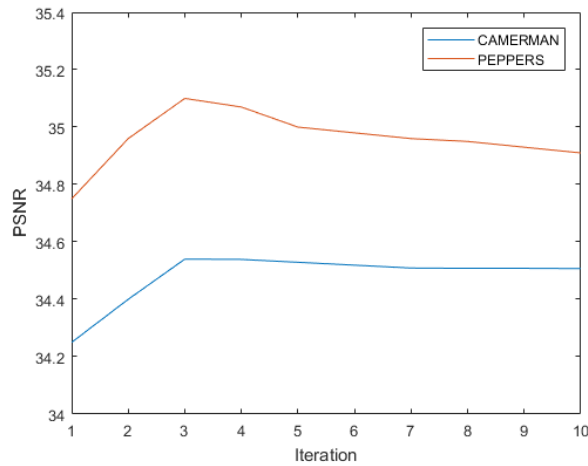


**Figure 13. Effects of the number of iterations on the CAMERAMAN and PEPPERS Images.**

Image	$\sigma_n$ (Noise Level)	Method [18]		Method [19]		Method [6]		Method [21]		Method [11]		Proposed	
		PSNR	FSIM	PSNR	FSIM	PSNR	FSIM	PSNR	FSIM	PSNR	FSIM	PSNR	FSIM
CAMERAMAN	10	34.20	0.87	33.36	0.77	34.23	0.83	34.33	0.87	34.35	0.88	<b>34.50</b>	<b>0.89</b>
	30	30.80	0.79	31.00	0.77	<b>31.40</b>	<b>0.80</b>	31.05	0.75	31.22	0.77	31.20	0.77
	50	28.80	0.61	<b>30.00</b>	<b>0.76</b>	28.90	0.57	29.62	0.66	29.60	0.66	29.90	0.68
LENA	10	34.80	0.96	35.10	0.94	35.60	0.96	<b>36.07</b>	<b>0.98</b>	36.00	0.98	36.03	0.97
	30	31.00	0.88	31.30	0.91	30.50	0.85	31.39	0.95	31.35	0.95	<b>31.70</b>	<b>0.95</b>
	50	28.50	0.72	29.3	0.84	28.10	0.68	29.07	0.92	28.96	0.92	<b>29.15</b>	<b>0.93</b>
PEPPERS	10	33.30	0.95	34.30	0.92	35.00	0.97	35.03	0.95	35.01	0.95	<b>35.10</b>	<b>0.97</b>
	30	<b>30.80</b>	0.87	30.40	0.89	31.20	0.87	30.40	0.87	30.45	0.89	30.50	<b>0.89</b>
	50	28.50	0.70	<b>29.50</b>	<b>0.88</b>	28.83	0.70	29.33	0.81	29.34	0.82	29.30	0.81
Mandrill	10	32.01	0.83	32	0.82	32.10	0.85	32.15	0.86	<b>32.20</b>	0.86	32.19	<b>0.87</b>
	30	29.50	0.75	29.45	0.74	29.78	0.75	29.85	0.76	29.95	0.76	<b>29.96</b>	<b>0.76</b>
	50	27.85	0.64	27.71	0.64	27.86	0.66	27.90	0.69	27.92	0.69	<b>27.95</b>	<b>0.70</b>
Boats	10	34.20	0.95	35	0.92	35.45	0.95	35.99	<b>0.97</b>	35.84	0.97	<b>36</b>	0.96
	30	30.56	0.87	31	0.90	30.35	0.83	31.35	0.94	31.21	0.93	<b>31.50</b>	<b>0.95</b>
	50	28.10	0.70	<b>29.10</b>	0.82	28.05	0.67	29	0.94	28.64	0.90	28.61	<b>0.89</b>
Average	-	30.92	0.80	31.23	0.83	31.15	0.80	31.50	0.86	31.46	0.864	<b>31.57</b>	<b>0.866</b>

**Table 3. The results of different methods on standard test images**



a) Original Image



b) Noisy Image



c) Method [18]



d) Method [19]



e) Method [6]



f) Method [21]



g) Method [11]



h) Proposed Method

.Figure 14. The results of different methods on CAMERAMAN with standard deviation of 10 in dB



a) Original Image



b) Noisy Image



c)  $k=1$ , PSNR=30.09



d)  $k=2$ , PSNR=31.8



e)  $k=3$ , PSNR=31.4



f)  $k=4$ , PSNR=31.02



g) Global, PSNR=30.75



h) Proposed, PSNR=33.61

**Figure 15. The results of the proposed method with different sparsities and in general on a noisy CAMERAMAN image with a standard deviation of 25 in dB.**

Time(second)	Method
11.21	Proposed Method
13.85	Method [19]
38.66	Method [18]
27.25	Method [6]
33.56	Method [21]
11.43	Method [11]

**Tabel 4. Runtime of different methods**

## 5. Conclusion

In this paper, a localized AWGN noise reduction method based on SVD is presented. In this method, using a low frequency component of noisy image and image gradient, a TI image is created which uses its data to adaptive optimal low rank approximation of each patch and the high frequency component of the noisy image will be input of proposed algorithm. To eliminate the noise of each patch from the high frequency component image, the corresponding patch is extracted in the TI image. If the average of the gradient of the patch exceeds the average gradient of the total TI image, the patch belongs to the textured parts of the image and therefore, using the answer to the optimization problem, it should be reconstructed. Otherwise, the patch belongs to the smooth areas that are reconstructed with less sparsity. This is done for all image patches to create a high frequency component of denoised image. The combination of the high-frequency component of denoised image and the low-frequency component of the noisy image make the output image of the algorithm. In the proposed method, the use of adaptive basis of signal representation and ideas such as patch labeling and the adaptive determination of the sparsity of each patch in the SVD domain, have caused that the proposed method, in addition to proper quality and accuracy, have an acceptable speed and computational complexity.

## References

1. Rudin, L.I., S. Osher, and E. Fatemi, *Nonlinear total variation based noise removal algorithms*. Physica D: nonlinear phenomena, 1992. **60**(1-4): p. 259-268.
2. McAndrew, A., *An introduction to digital image processing with matlab notes for scm2511 image processing*. School of Computer Science and Mathematics, Victoria University of Technology, 2004. **264**(1): p. 1-264.
3. Mousavi, B.S., F. Soleymani, and N. Razmjooy, *Color image segmentation using neuro-fuzzy system in a novel optimized color space*. Neural Computing and Applications, 2013. **23**(5): p. 1513-1520.
4. Razmjooy, M. and M. Ramezani. *Model Order Reduction based on meta-heuristic optimization methods*. in *1st International Conference on New Research Achievements in Electrical and Computer Engineering Iran*. 2016.
5. Razmjooy, N., et al., *Automatic selection and fusion of color spaces for image thresholding*. Signal, Image and Video Processing, 2014. **8**(4): p. 603-614.
6. Razmjooy, N., et al. *Image Thresholding Optimization Based on Imperialist Competitive Algorithm*. in *3rd Iranian Conference on Electrical and Electronics Engineering (ICEEE2011)*. 2011.

7. Zhang, X., et al., *Compression artifact reduction by overlapped-block transform coefficient estimation with block similarity*. IEEE transactions on image processing, 2013. **22**(12): p. 4613-4626.
8. Khan, A., et al., *Image de-noising using noise ratio estimation, K-means clustering and non-local means-based estimator*. Computers & Electrical Engineering, 2016. **54**: p. 370-381.
9. Takeda, H., S. Farsiu, and P. Milanfar, *Kernel regression for image processing and reconstruction*. IEEE Transactions on image processing, 2007. **16**(2): p. 349-366.
10. Fan, L., et al., *Nonlocal image denoising using edge-based similarity metric and adaptive parameter selection*. Science China Information Sciences, 2018. **61**(4): p. 049101.
11. Shanthi, S.A., C.H. Sulochana, and T. Latha, *Image denoising in hybrid wavelet and quincunx diamond filter bank domain based on Gaussian scale mixture model*. Computers & Electrical Engineering, 2015. **46**: p. 384-393.
12. Chen, M., et al. *An OCT image denoising method based on fractional integral*. in *Optical Coherence Tomography and Coherence Domain Optical Methods in Biomedicine XXII*. 2018. International Society for Optics and Photonics.
13. Guo, Q., et al., *An efficient SVD-based method for image denoising*. IEEE transactions on Circuits and Systems for Video Technology, 2015. **26**(5): p. 868-880.
14. Aharon, M., M. Elad, and A. Bruckstein, *K-SVD: An algorithm for designing overcomplete dictionaries for sparse representation*. IEEE Transactions on signal processing, 2006. **54**(11): p. 4311-4322.
15. Elad, M. and M. Aharon, *Image denoising via sparse and redundant representations over learned dictionaries*. IEEE Transactions on Image processing, 2006. **15**(12): p. 3736-3745.
16. Mallat, S. and G. Yu, *Super-resolution with sparse mixing estimators*. IEEE transactions on image processing, 2010. **19**(11): p. 2889-2900.
17. Jiang, L., X. Feng, and H. Yin, *Structure and texture image inpainting using sparse representations and an iterative curvelet thresholding approach*. International Journal of Wavelets, Multiresolution and Information Processing, 2008. **6**(05): p. 691-705.
18. Kalantari, S. and M.J. Abdollahifard, *Optimization-based multiple-point geostatistics: A sparse way*. Computers & geosciences, 2016. **95**: p. 85-98.
19. Pizurica, A. and W. Philips, *Estimating the probability of the presence of a signal of interest in multiresolution single-and multiband image denoising*. IEEE Transactions on image processing, 2006. **15**(3): p. 654-665.
20. Zhang, J., et al., *Image restoration using joint statistical modeling in a space-transform domain*. IEEE Transactions on Circuits and Systems for Video Technology, 2014. **24**(6): p. 915-928.
21. Jiang, J., L. Zhang, and J. Yang, *Mixed noise removal by weighted encoding with sparse nonlocal regularization*. IEEE transactions on image processing, 2014. **23**(6): p. 2651-2662.
22. Dabov, K., et al., *Image denoising by sparse 3-D transform-domain collaborative filtering*. IEEE Transactions on image processing, 2007. **16**(8): p. 2080-2095.
23. Dabov, K., et al., *Image denoising with shape-adaptive principal component analysis*. Department of Signal Processing, Tampere University of Technology, France, 2009.
24. He, Y., et al., *Adaptive denoising by singular value decomposition*. IEEE Signal Processing Letters, 2011. **18**(4): p. 215-218.
25. Dong, W., G. Shi, and X. Li, *Nonlocal image restoration with bilateral variance estimation: a low-rank approach*. IEEE transactions on image processing, 2012. **22**(2): p. 700-711.
26. Razmjoooy, N., S.S. Naghibzadeh, and B.S. Mousavi, *Automatic redeye correction in digital photos*. International Journal of Computer Applications, 2014. **95**(9).
27. Razmjoooy, N., F.R. Sheykhahmad, and N. Ghadimi, *A hybrid neural network–world cup optimization algorithm for melanoma detection*. Open Medicine, 2018. **13**(1): p. 9-16.

28. Mallat, S., *A Wavelet Tour of Signal Processing: The Sparse Way* (Academic, Burlington, MA). 2008.
29. Starck, J.-L., E.J. Candès, and D.L. Donoho, *The curvelet transform for image denoising*. IEEE Transactions on image processing, 2002. **11**(6): p. 670-684.
30. Mallat, S. and G. Peyré, *A review of bandlet methods for geometrical image representation*. Numerical Algorithms, 2007. **44**(3): p. 205-234.
31. Do, M.N. and M. Vetterli, *The contourlet transform: an efficient directional multiresolution image representation*. IEEE Transactions on image processing, 2005. **14**(12): p. 2091-2106.
32. Bleistein, N., R.A. Handelsman, and J. Lew, *Functions whose Fourier transforms decay at infinity: An extension of the Riemann-Lebesgue lemma*. SIAM Journal on Mathematical Analysis, 1972. **3**(3): p. 485-495.
33. Eckart, C. and G. Young, *The approximation of one matrix by another of lower rank*. Psychometrika, 1936. **1**(3): p. 211-218.